REFLECTION, DIFFRACTION AND RESOLUTION

T. Kaschwich, H. Gjøystdal, I. Lecomte, and E. Iversen

email: *tina@norsar.no*
keywords: *Modelling, Resolution, Kirchhoff-type*

ABSTRACT

Seismic "reflection" data contain two types of coherent events generated from the subsurface discontinuities: specular reflections and diffractions. Most seismic data processing is tuned to imaging and enhancing reflected waves, which carry most of the information about the actual subsurface. Diffractions are generated by local discontinuities which act like point sources. Therefore, the presence of diffractions can indicate faults or fractures, which are important in, e.g., carbonate environments, where locating fractures and their orientation is of major importance for reservoir production. Ray tracing in its standard forms is not able to produce complete synthetic seismograms, i.e., including diffractions. In this paper we investigate the impact of diffractions on pre-stack depth migration images and discuss some correlated resolution aspects. Furthermore, we present examples where we apply a ray-based approach to compute synthetic seismograms for both reflected and diffracted events. Finally, we document the applicability of the approach to different model types, e.g., isotropic and anisotropic media.

INTRODUCTION

Prestack depth migration (PSDM) should be the ultimate goal of seismic processing, producing angle-dependant depth images of the subsurface scattering properties. But the expected quality of PSDM images is constrained by many factors. Understanding all of these factors is necessary to improve depth imaging of geologic structures. In all PSDM approaches, e.g., Kirchhoff or wave-equation, migration always includes compensating for wave propagation in the overburden (back propagation, downward continuation, etc.), before focusing back the reflected/diffracted energy at each considered location in depth (imaging). Ideally, we would like to retrieve the reflectivity of the ground as detailed as possible to invert for the elastic parameters. But the waves perceive the reflectivity through "thick glasses," seeing blurred structures, and not necessarily all of them, depending on the illumination. Only a filtered version of the true reflectivity is therefore retrieved. Being able to estimate these filters, the so-called resolution is the key to a better understanding of the imaging results and improving them, either at an early stage by careful survey planning, or, possibly at a later stage, by properly tuning migration parameters.

Ray-based seismic modelling methods can be applied at various stages of the exploration and production process. The standard ray method has several advantages, e.g., computational efficiency and they provide us with physical insight that can not be obtained from a brute-force numerical solution. In addition ray tracing has an event-oriented nature, which means that specific arrivals of elementary waves (e.g., transmitted P and S waves, primary PP and PS reflected waves for selected horizons, multiples, etc.) can be labeled in synthetic seismograms or in computed sets of Green‘s function attributes. Comparisons with more complete (and much more time-consuming) techniques, like finite-difference schemes (FD), show that theoretical seismograms obtained by classical dynamic ray tracing (DRT) can be very qualified if the model is prepared with the necessary smoothness.

The main weakness of the ray method applied to complex geological structures is due to the fact that the calculations along each ray is "super-local", i.e., quite independent of the neighboring rays. One single ray

"sees" only the velocity and interface behavior exactly along the raypath, and thus the stability across the rays depends on the assumption that these parameters are fairly representative for neighboring rays (at least within the Fresnel zone). As an alternative to classical two-point ray tracing, Vinje et al. (1993, 1996a,b) and Gjøystdal et al. (2002, 2007) developed the wavefront construction method (WFC), which is a more robust ray tracing technique adapting the ray density to the model and interpolating the ray attributes. The reason for enhanced robustness lies in the fact that a continuous representation of the wavefront, with sufficiently dense sampling of ray points and slowness vectors, is established by interpolation after each time step. However, this method only partly solves the problem of lack of ray penetration into shadow zones and fails in the vicinities of caustics.

Seismic reflection data contain two types of coherent events generated from the subsurface discontinuities: specular reflections and diffractions (Krey, 1952; Hagedoorn, 1954). Most seismic data processing is tuned to imaging and enhancing reflected waves, to interpret structural and stratigraphic features of the subsurface. The value of diffracted waves, however, should not be underestimated (Klem-Musatov, 1994; Khaidukov et al., 2004). Specular reflections are generated by interfaces with impedance contrasts, however, diffractions are generated by local discontinuities which act like point sources. When seismic exploration focuses on identifying small subsurface features (such as faults, fractures, channels, and rough edges of salt bodies) or abrupt changes in seismic reflectivity (such as those caused by fluid presence or fluid flow during reservoir production), the diffracted waves contain valuable information.

To obtain more accurate and realistic reflection seismograms than those obtained by classical ray tracing in case of complex geological structures, Kaschwich et al. (2009) presented a ray-based approach combining classical Kirchhoff demigration (Tygel et al., 1994, 2000) and the PSDM simulator approach of NORSAR (SimPLI technology; Lecomte, 2006, 2008a).

In this paper, we present several examples to demonstrate the influence of missing diffractions on the resolution of the final prestack depth migrated image using our new approach to compute synthetic seismograms (see also Kaschwich and Lecomte, 2010).

DEMIGRATION USING A PSDM PREDICTOR

Demigration is a seismic forward-modelling scheme based on seismic imaging; it is a ‘forward‘ technique, due to the fact that a velocity model needs to be specified (see scheme in Figure 1). On the other hand, demigration can be considered as the inverse of migration (Hubral et al., 1996; Tygel et al., 1996; Santos et al., 2000).

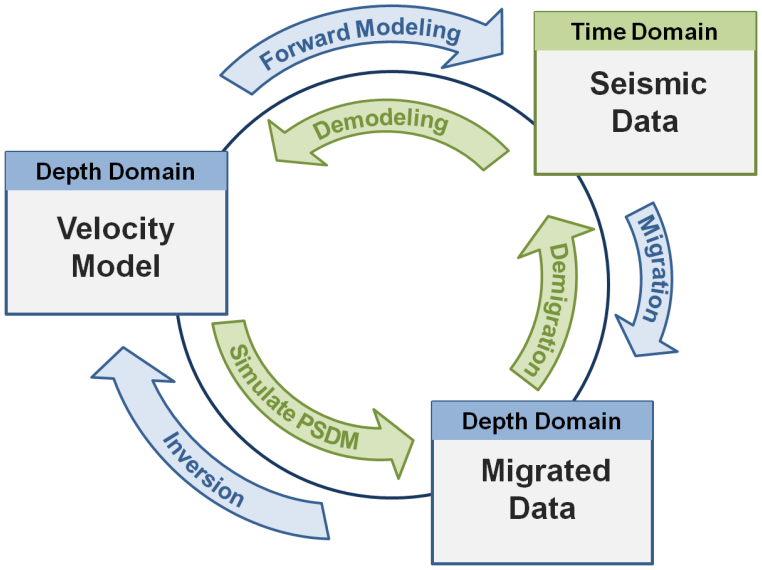

Figure 1: Cycle of Kirchhoff-based imaging operations (taken from Riede, 2002).

Given a seismic model with explicit reflectors, the true amplitude reflector image can directly be constructed from a given reflector and a chosen wavelet. Then in a second step, the true-amplitude demigration can be performed, thus offering a new seismic modelling method, i.e., modelling by demigration.
In this paper, we use an alternative approach to calculate the artificial migrated image based on a ray-based PSDM simulator called in the following SimPLI (Simulated Prestack Local Imaging; Lecomte et al., 2003; Lecomte, 2004; Lecomte and Pochon-Guerin, 2005; Lecomte, 2006, 2008a). SimPLI directly produces simulated prestack depth migrated images of a given reservoir model, without generating synthetic traces and processing them. This approach makes use of the PSDM resolution (inverse problem), i.e., applying the calculated ray-based point-spread functions (PSF; Lecomte and Gelius, 1998) in a background velocity model to the reflectivity of a superimposed target (e.g., reservoir). This is done by either convolution in the depth domain, or multiplication in the scattering-wavenumber domain, and using fast FT (FFT) to perform the depth-to/from-wavenumber conversions. SimPLI acts as a signal- or image-processing method, distorting the actual reflectivity to reproduce the effects of seismic imaging. This is comparable to what is done in PSDM, where a seismic data set is used to retrieve the unknown reflectivity (only a filtered version, as suggested earlier). This distorted reflectivity is superimposed by PSDM to the (smooth) background velocity field used for the propagation effects. In the simulator approach, which is a modelling one, we know the reflectivity in depth, so there is no need for the back propagation of the migration method, but we simulate instead the focusing effect (imaging) by distorting the true reflectivity according to the PSF. Other approaches are also possible (Toxopeus et al., 2008), but the ray approach provides a flexible, interactive and robust concept for PSF estimation (Gjøystdal et al., 2007; Lecomte, 2008b).
Consider the model in Figure 2. It consists of a slightly undulated reflector that separates two homogeneous isotropic layers. P-velocities above and below the horizon are 2000 and 2500 m/s respectively, P/S velocity ratio is 1.7, and density is 2.0 g/cm^3. Now we consider a common shot survey along a line in the x direction, with shots between 8 and 14 km and a spacing of 100 m. The receiver line is 4 km long and the spacing is 100 m. For illustration, Figure 2 shows all shot positions and some raypaths resulting from WFC.

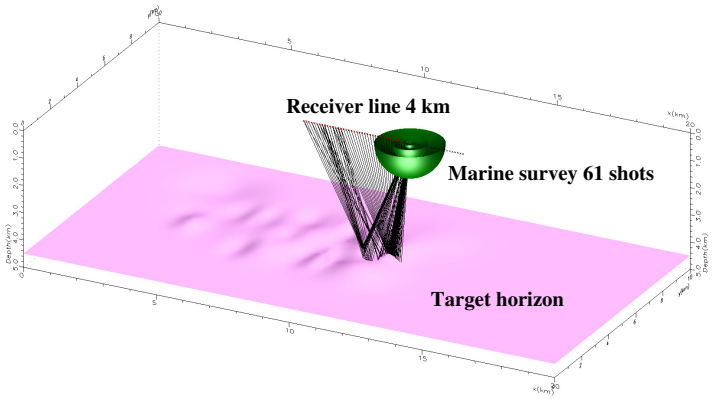

Figure 2: First example consists of an undulated reflector that separates two homogeneous isotropic layers.

For the given survey two different data sets were computed: one using the NORSAR-3D standard ray tracing approach and the second by applying the modelling by demigration technique. The new approach uses ray-based one-way Green's functions (GF) calculated by NORSAR-3D. Figure 3 shows the different PSDM results calculated for the given structure for these two different data sets. By quantitatively comparing both seismic sections it can be seen that the reflector is well imaged in both cases. However, typical deficiencies that can be observed in migrated sections obtained by the DRT data set (Figure 3a) are the residual noise where the undulations of the structure are located. The standard ray-tracing seismograms have some unrealistically high amplitudes close to the cusps of caustics, and a lack of a gradual decay in the form of diffracted energy. On contrary, the PSDM result obtained by the modelling by demigration input data (Figure 3b) gives a good image of the subsurface structure and reveals much less noise.

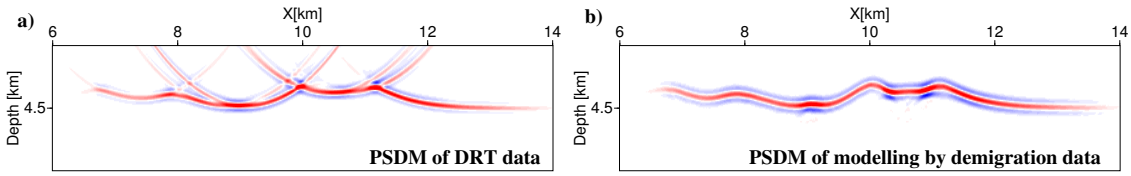

Figure 3: PSDM results for data input obtained by different modelling techniques: (a) Standard ray-tracing and (b) modelling by demigration.

RESOLUTION AND POINT SPREAD FUNCTION

A point spread function is the PSDM response of a point scatterer and thus the obtained image of the PSF is controlled by various factors. Assuming a complex velocity model, all effects including acquisition geometry, velocity model, pulse, wave type, etc., need to be taken into account. For example, using the Marmousi model as a background model, the calculated PSFs show significant variations for a few points at one lateral position and at different depths (Figure 4). Elastic quantities and survey geometry are taken from Versteeg (1994).

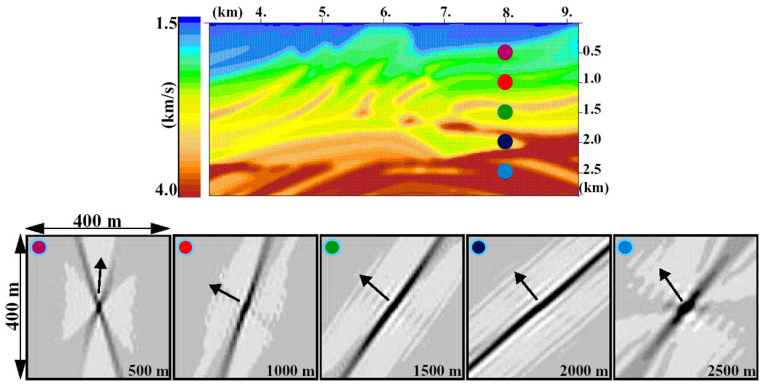

Figure 4: Marmousi model. (a) PSDM background velocity model with five selected locations in depth for one lateral position (colored disks). (b) Calculated PSF at each of the five selected locations for a $5 - 60$ Hz frequency band and an incident angle range of $0 - 10°$ (taken from Lecomte, 2008b).

To better understand what happens in PSDM, we start with the elementary problem of imaging point scatterers. However, the diffraction points in the subsurface, acts as secondary sources when first illuminated by a seismic source. A background velocity field is needed to compensate for wave propagation effects between sources and receivers down to each image point. The most relevant quantity for migration is traveltime, i.e., the migration process must be able to locate back in depth backscattered energy recorded in time. For two different survey types and one source-receiver couple, Figure 5a and 5b illustrate PSDM images. For a time recording of backscattered energy at R due to source at S, so-called scattering traveltimes $t_{SR} = t_S + t_R$ are needed at each image point to relate seismic energy recording time to depth locations. Here, t_S and t_R are the traveltime from the source/receiver to the image point, respectively. The isolines of t_{SR} are called scattering isochrones and are elliptic in the homogeneous isotropic case. Some migration methods will explicitly calculate t_{SR} in the chosen velocity model (Kirchhoff or diffraction stack), while others will do so implicitly when forward/back propagating wavefields in that velocity field, but in all cases, the scattering traveltime t_{SR} is the key to the depth imaging process as well as in the presented demigration process.

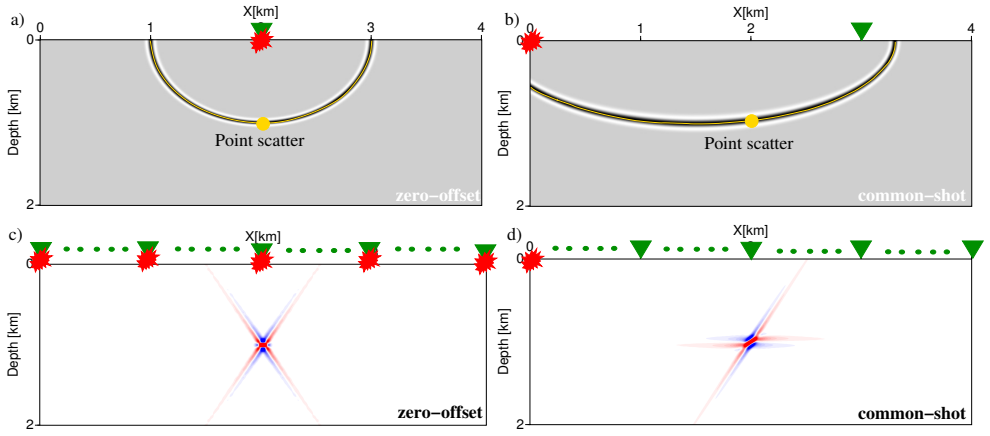

Figure 5: Scattering isochrones and PSDM. The background velocity model is homogeneous and isotropic. A point scatterer is located at the center of the image (yellow disk). Both a zero-offset survey (shot/receiver positions spread over 4 km) and a common-shot survey (one shot at 0 km and receivers along the same 4 km) are considered. (a) Zero-offset: PSDM image attached to one shot/receiver couple, i.e., the one just above the point scatterer. (b) Common-shot: PSDM image attached to one receiver at 3 km. (c) Zero-offset: PSDM image attached to the whole zero-offset survey. (d) Common-shot: PSDM image attached to the whole common shot acquisition.

EXAMPLE

In this section we show different applications of our approach to compute synthetic seismograms and compare the migrated images with standard ray-tracing results. The first example focus on the resolution effect observed by neglecting the diffraction events. Furthermore, this example is used to demonstrate the resolution changes due to applied migration aperture. Finally, we investigate the influence of different model types (i.e., isotropic or anisotropic) used for PSDM and thus the consequences of ignoring anisotropy inherent in the subsurface structures.

A square pattern

Consider the model in Figure 6. It consists of one plane horizon that separates two isotropic layers. The upper layer is assumed to be homogeneous whereas the lower layer shows a systematic square pattern for the P-wave velocity. The P-velocity above the horizon is 2000 m/s and the velocity value in the lower layer alternate between 2000 m/s and 2500 m/s, P/S velocity ratio is 1.7, and density is 2.0 g/cm^3. The seismic data was generated for a zero-offset survey with shot/receiver spacing of 20 m and the shot/receivers are located between 4 and 6 km in both directions x and y. In this example a 30-Hz zero-phase Ricker wavelet was used as the source pulse.
Figure 7a shows the xy view of the reflectivity in the target area. The pattern defines areas where seismic energy is reflected in red and white indicates areas with a zero reflection coefficient. Using the SimPLi approach (e.g., Lecomte et al., 2003; Lecomte, 2004, 2008a) we obtain the simulated seismic response for the zero-offset survey as given in Figure 7b. Here we see a similar pattern as the reflectivity grid but as expected less sharp contours of the single rectangle due to the assumed survey and migration process. Finally, Figures 7c and d give the resulting PSDM images using the DRT seismograms and the modelling by demigration seismic inputs, respectively. This example reveals the deficiency of standard ray tracing as the resulting pattern appears to be smeared and not well defined. Basically this blurring effect appears because of the lack of diffractions in the seismic data. In comparison the modelling by demigration input gives a clean picture of the reflectivity on the target reflector.

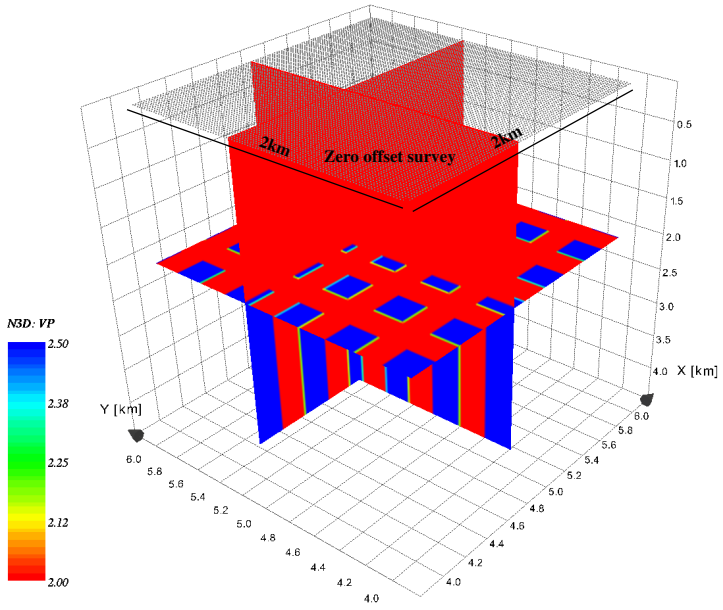

Figure 6: Square pattern reflectivity distribution on a horizontal layer and the assumed zerooffset survey.

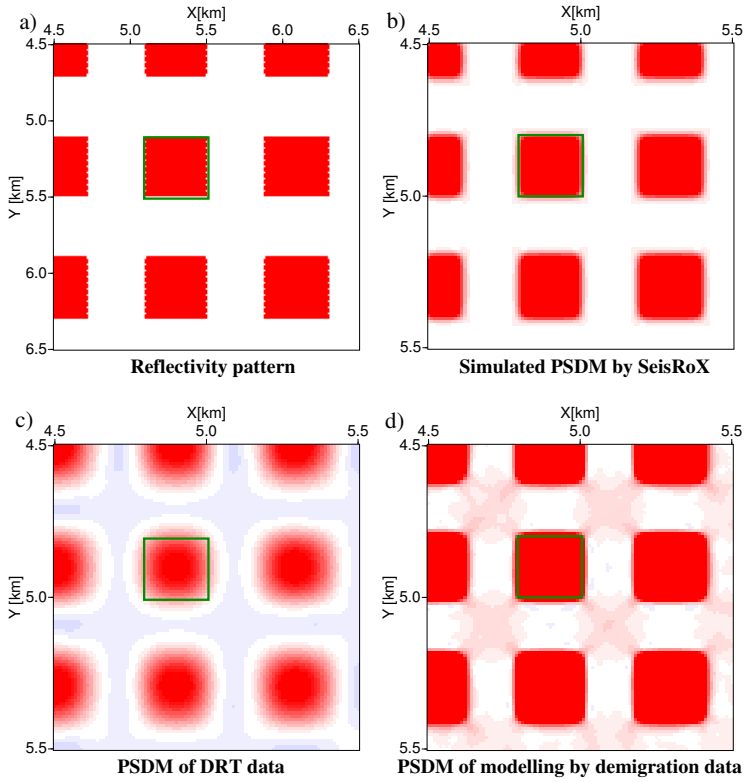

Figure 7: Comparison between reflectivity and PSDM results: (a) Reflectivity pattern on a plane reflector, (b) simulated PSDM results by SimPLI, (c) PSDM results using the DRT seismogram generated by NORSAR-3D, (d) PSDM result obtained by using modelling by demigration data.

In the following we are using the pattern model (Figure 6) to demonstrate the impact of the chosen migration aperture. Figure 8 shows the corresponding PSFs for two different cases, full aperture and a restriction to 300 m. The full aperture PSF was used to obtain the simulated seismic in Figure 7b. If the subsurface target is assumed to be flat, the resulting seismic for both case show nearly the same PSDM image (see Figure 9c and 9d). However, comparing the images for the pattern model (Figure 9) it is evident that the 300 m aperture gives a blurred result at the edges of each rectangular (Figure 9b). Using the full migration aperture gives a well defined boundary of each reflecting pattern at the target horizon (Figure 9a).

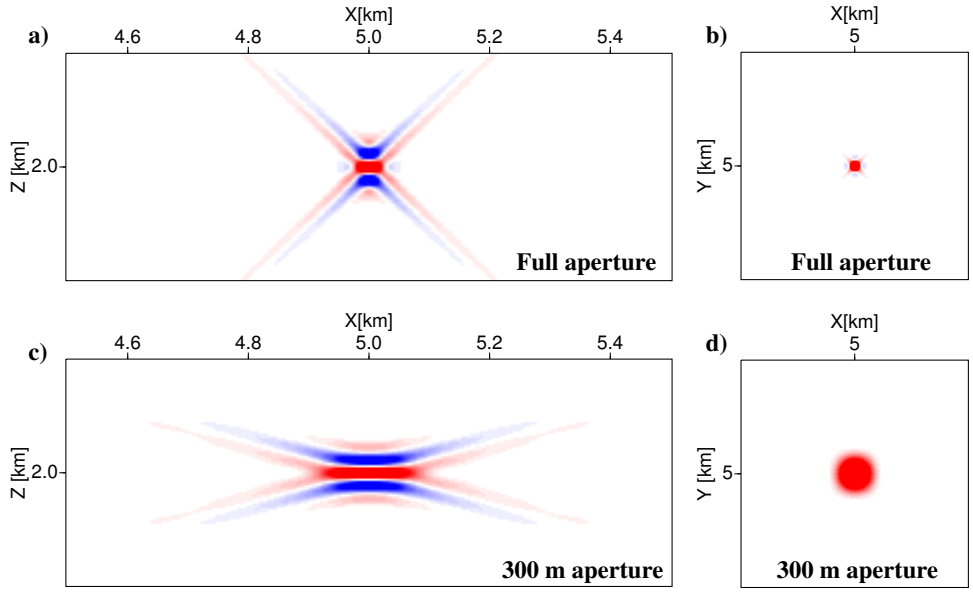

Figure 8: Influence of the migration aperture on the resulting PSFs, PSF for the full aperture xz view (a) and xy view (b), compared to a 300-m aperture xz view (c) and xy view (d).

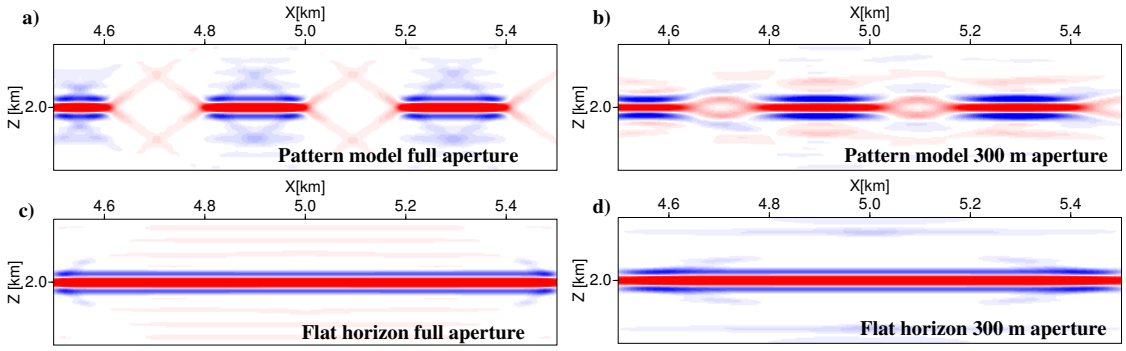

Figure 9: Resulting seismic images, for the full-aperture: pattern model (a) and flat horizon (c), and for the 300-m migration aperture: pattern model (b) and flat horizon (d).

Anisotropic salt model

Shales comprise a large proportion of most sedimentary basins and form the seal and source rocks for many hydrocarbon reservoirs. Often shale formations are anisotropic and therefore, anisotropy is becoming an important issue in exploration and reservoir geophysics. The origin of seismic anisotropy in shales is non-

unique and may be attributed to several factors, e.g., including preferred orientation of clay platelets, micro-cracks, fine-layering and/or stress-induced anisotropy. Incorporating anisotropy into imaging algorithms will facilitate the correct positioning of the reservoir targets. Therefore, we present as a final example a model that consists of a salt structure/dome and several adjacent shale layers (Figure 10). The P-wave velocity is given in Figure 10a (a corresponding S-wave velocity field is defined, but not further taken into account in this experiment). The Thomsen parameters ϵ and δ are given in Figure 10c and 10d, respectively. The anisotropy is assumed to be tilted transversely isotropic (TTI), the axis of symmetry is a smooth field and the assumed angle corresponds to an axis which is approximately perpendicular to the shale layers.

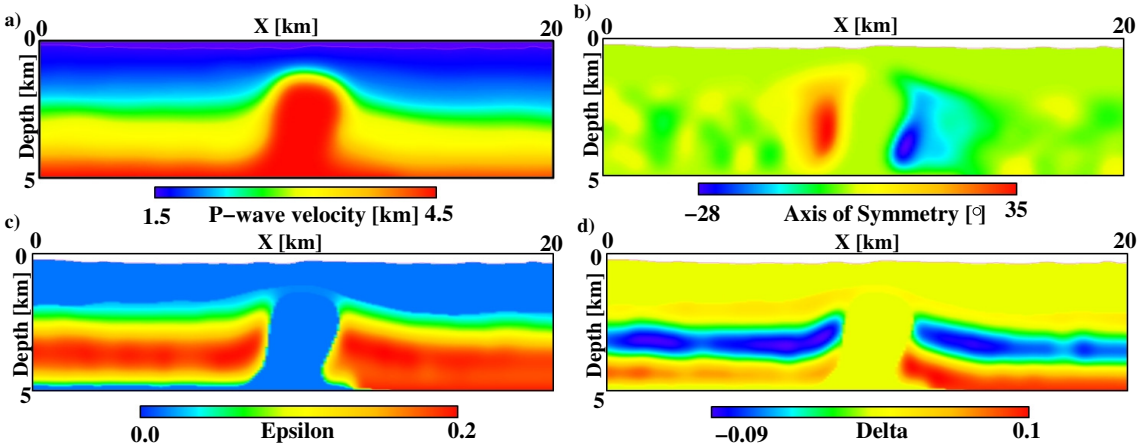

Figure 10: The anisotropic salt model: (a) the P-wave velocity, (b) the axis of symmetry distribution, the Thomsen parameter ϵ (c) and δ (d).

The point scatterers are located around the salt dome inherent in the subsurface model (Figure 11). For these positions the PSFs are computed using the approach described above. Using our modelling-by-demigration approach applied on these PSFs we obtain a synthetic data set containing the corresponding diffractions for a marine-type common shot survey. The 81 shots are located between 6 km and 14 km, shot spacing was 100 m and the 151 receivers had a spacing of 20 m.

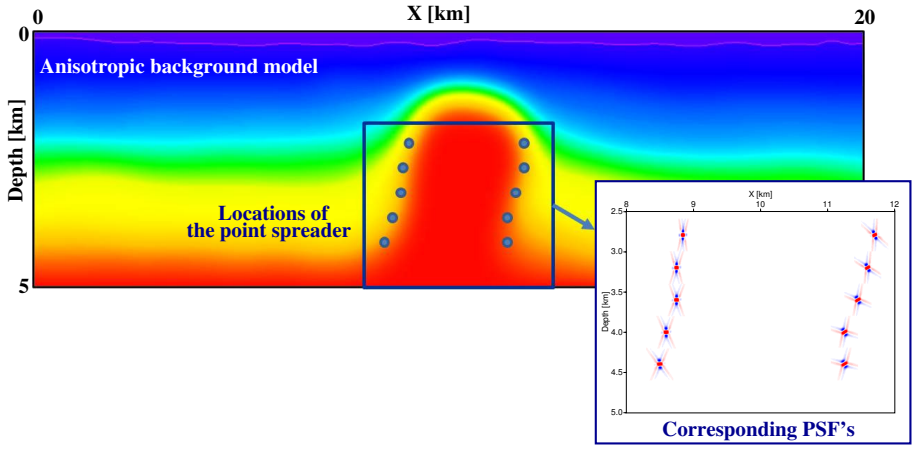

Figure 11: Location of 10 point scatterers surrounding the salt dome and the corresponding PSFs calculated by SimPLI.

Figure 12 shows synthetic seismograms for 4 different shot positions obtained by the presented modelling-by-demigration approach. The Green's functions needed for the demigration process were computed in the anisotropic background model given in Figure 10.

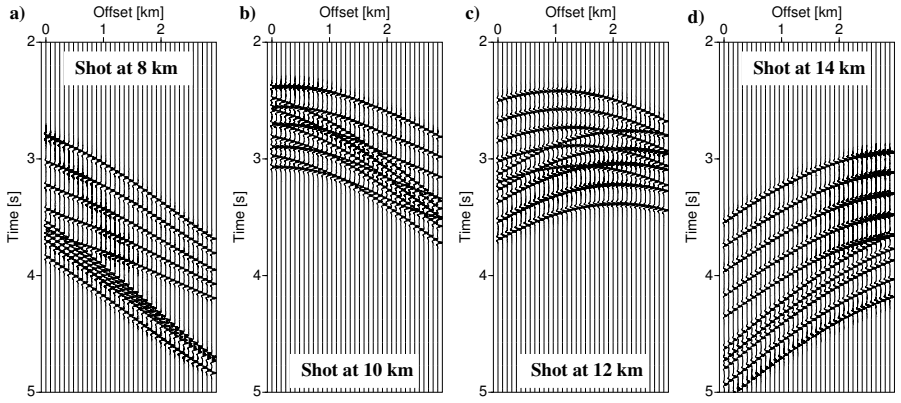

Figure 12: Synthetic data for 4 shot positions (a) at 8 km, (b) at 10km, (c) 12 km and (d) at 14 km.

In the following we want to investigate the influence of the assumed background model for the migration process. The synthetic data (Figure 12) is computed considering an anisotropic background model with a tilted symmetry axis. However, we now migrate this input data assuming 3 types of subsurface models: for the isotropic version we omit the anisotropy parameter, ϵ, δ, and the axis of symmetry. Furthermore, we obtain a vertical transversely isotropic (VTI) media by ignoring all variations in the axis of symmetry. The resulting PSDM images are given in Figure 13.

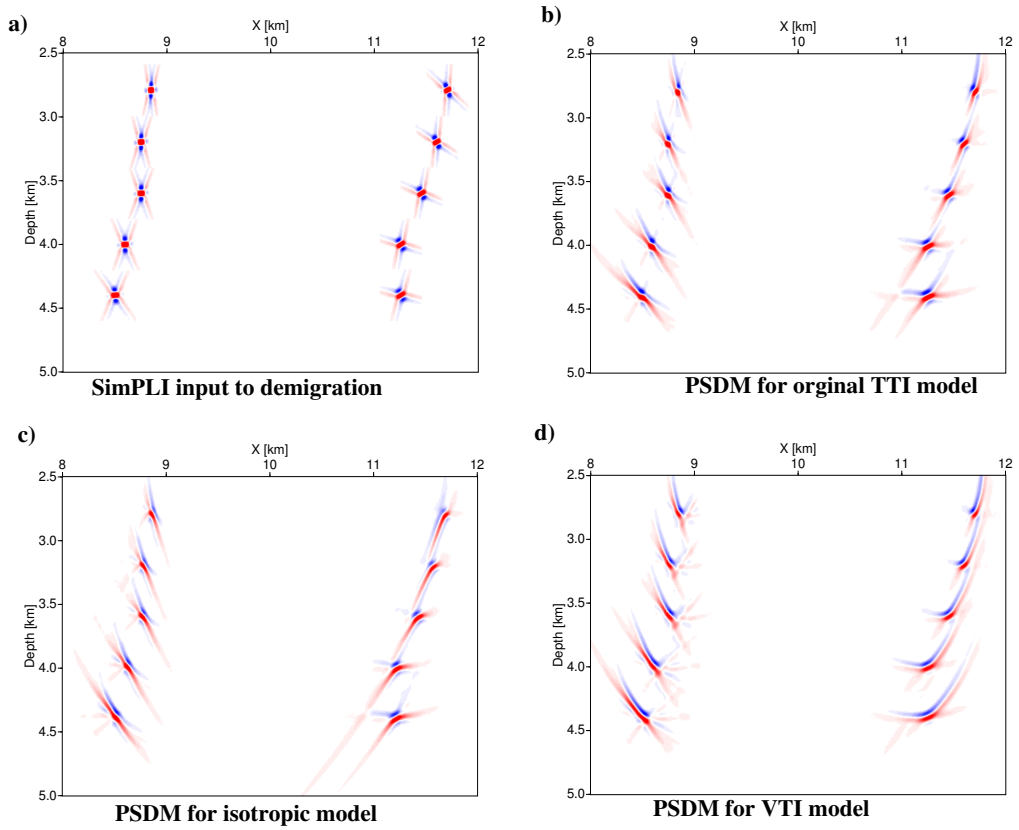

Figure 13: PSDM results: (a) PSFs computed by SimPLI, (b) PSDM image using the correct TTI background model, (c) PSDM result using the isotropic version of the saltmodel and (d) PSDM image using GF's calculated for the VTI model.

Comparing the different PSDM results (Figure 13b-d) with the originally calculated PSFs (Figure 13a) reveals a lack of focussing for the VTI background model (Figure 13c). As expected the TTI background model gives the best imaging result, however also here we observe some residual 'noise'. This may be explained by the lack of curvature of the PSFs as our approach obtains the ray-based PSF with a local plane-wave approximation. In comparison to the VTI background for our survey configuration the isotropic version gives rather good results.

CONCLUSIONS

More and more seismic exploration focuses on identifying small subsurface features or small changes in seismic reflectivity, where diffracted waves contain valuable information. Especially in ray modelling the lack of diffractions has a significant impact on the obtained PSDM result particularly with respect to lateral resolution. The presented modelling by demigration approach turns out to be an effective technique to overcome some of the limits of ray theory, since it dramatically reduces the need for reflector smoothness, thereby modelling both edge and caustic diffractions. Although more time consuming, it is quite feasible to perform modelling by demigration in three dimensions today, having an efficient wavefront construction tracer running in parallel, even on small clusters. Kaschwich et al. (2009) showed that the result by the new SimPLI/modelling-by-migration approach gives similar results as the classical Kirchhoff modelling. However, Kirchhoff modelling considers only one horizon at a time, while the demigration approach is a volume method an thus all reflectors can be considered at once.

ACKNOWLEDGMENTS

We thank our research partners of the Wave Inversion Technology (WIT) Consortium, especially Martin Tygel, for fruitful discussions.

REFERENCES

Gjøystdal, H., Iversen, E., Laurain, R., Lecomte, I., Vinje, V., and Åstebøl, K. (2002). Review of ray theory applications in modelling and imaging of seismic data. *Studia geophysica et geodetica*, 46:113–164.

Gjøystdal, H., Iversen, E., Lecomte, I., Kaschwich, T., Drottning, Å., and Mispel, J. (2007). Improved applicability of ray tracing in seismic acquisition, imaging, and interpretation. *Geophysics*, 72:SM261–SM271.

Hagedoorn, J. (1954). A process of seismic reflection interpretation. *Geophys. Prosp.*, 2:85–127.

Hubral, P., Schleicher, J., and Tygel, M. (1996). A unified approach to 3-D seismic reflection imaging-Part I: Basic concepts. *Geophysics*, 61:742–758.

Kaschwich, T. and Lecomte (2010). Improved Ray-based Seismograms by Combining Modeling by Demigration with a Prestack Depth Migration Simulator. *eage71*, page C041.

Kaschwich, T., Lecomte, I., Gjøystdal, H., Iversen, E., and Tygel, M. (2009). Advanced ray-based synthetic seismograms. *13th Annual Report of the Wave Inversion Technology (WIT) consortium*, pages 158–171.

Khaidukov, V., Landa, E., and Moser, T. (2004). Diffraction imaging by focusing-defocusing: An outlook on seismic superresolution. *Geophysics*, 69:1478–1490.

Klem-Musatov, K. D. (1994). *Theory of seismic diffractions*, volume No. 1: SEG. Open File Publications.

Krey, T. (1952). The significance of diffraction in the investigation of faults. *Geophysics*, 17:843–858.

Lecomte, I. (2004). Simulating Prestack Depth Migrated Sections. *66th Mtg. Eur. Assn. of Expl. Geophys., Expanded Abstracts*, P071.

Lecomte, I. (2006). Fremgangsmåte for simulering av locale prestakk dypmigrerte seismiske bilder. Norway patent #322089.

Lecomte, I. (2008a). Method simulating local prestack depth migrated seismic images. US patent #7,376,539.

Lecomte, I. (2008b). Resolution and illumination analyses in PSDM: A ray-based approach. *The Leading Edge*, 27(5):650–663.

Lecomte, I. and Gelius, L. J. (1998). Have a look at the resolution of prestack depth migration for any model, survey and wavefields. *68th Ann. Internat. Mtg., Soc. of Expl. Geophys., Expanded Abstracts*, SP 2.3.

Lecomte, I., Gjøystdal, H., and Drottning, Å. (2003). Simulated Prestack Local Imaging: a robust and efficient interpretation tool to control illumination, resolution, and timelapse properties of reservoirs. *73th Ann. Internat. Mtg., Soc. of Expl. Geophys., Expanded Abstracts*, pages 1525–1528.

Lecomte, I. and Pochon-Guerin, L. (2005). Simulated 2D/3D PSDM images with a fast, robust, and flexible FFT-based filtering approach. *75th Ann. Internat. Mtg., Soc. of Expl. Geophys., Expanded Abstracts*, pages 1810–1813.

Riede, M. (2002). *Kirchhoff Migration, Demigration and Seismic Modeling by Demigration*. Logos Verlag Berlin.

Santos, L. T., Schleicher, J., Hubral, P., and Tygel, M. (2000). Seismic modeling by demigration. *Geophysics*, 65(4):1281–1289.

Toxopeus, G., Thorbecke, J., Wapenaar, K., Petersen, S., Slob, E., and J., F. (2008). Simulating migrated and inverted seismic data by filtering a geologic model. *Geophysics*, 73:T1–T10.

Tygel, M., Schleicher, J., and Hubral, P. (1994). Kirchhoff-Helmholtz theory in modelling and migration. *J. Seis. Expl.*, 2:203–214.

Tygel, M., Schleicher, J., and Hubral, P. (1996). A unified approach to 3-D seismic reflection imaging- Part II: Theory. *Geophysics*, 61:759–775.

Tygel, M., Schleicher, J., Santos, L. T., and Hubral, P. (2000). An asymptotic inverse to the Kirchhoff-Helmholtz integral. *Inverse Problems*, 16:425–445.

Versteeg, R. (1994). The Marmousi experience: Velocity model determination on a synthetic complex data set. *The Leading Edge*, 13:927–936.

Vinje, V., Iversen, E., Åstebøl, K., and Gjøystdal, H. (1996a). Estimation of multivalued arrivals in 3D models using wavefront construction- Part I. *Geophys. Prosp.*, 44:819–842.

Vinje, V., Iversen, E., Åstebøl, K., and Gjøystdal, H. (1996b). Part II: Tracing and interpolation. *Geophys. Prosp.*, 44:843–858.

Vinje, V., Iversen, E., and Gjøystdal, H. (1993). Traveltime and amplitude estimation using wavefront construction. *Geophysics*, 58:1157–1166.